Radiologic Clinics of North America
Volume 39 • Number 6 • November 2001

HIGH-RESOLUTION CT OF ALVEOLAR FILLING DISORDERS

Kyung Soo Lee MD [1]

Eun A. Kim MD [1]

[1] Department of Radiology, Samsung Medical Center, Sungkyunkwan University School of Medicine, Seoul, Korea

Address reprint requests to
Kyung Soo Lee, MD
Department of Radiology
Samsung Medical Center
Sungkyunkwan University School of Medicine
50, Ilwon-Dong, Kangnan-Ku
Seoul 135-710
Korea
e-mail: kslee@smc.samsung.co.kr

Most diseases that cause increased lung density on chest radiograph involve the airspace and interstitium to a variable extent. It is helpful, however, to divide the lung diseases into three categories in the interpretation of high-resolution CT (HRCT).[45] The three categories are airspace filling process, interstitial process, and mixed airspace and interstitial process. Alveolar, or airspace, filling process refers to a condition in which the disease mainly affects the terminal airspaces.[24] Airspace filling process is characterized on CT by the presence of one or more fairly homogeneous areas of consolidation with little or no volume loss. The consolidation may be segmental, subsegmental, or lobular. The margin of the consolidation usually is defined poorly, except in the areas where the consolidation abuts the pleura. Air-containing bronchi or bronchioles (CT air bronchograms or air bronchiolograms, respectively) are seen frequently. Localized round areas of consolidation measuring 10 mm or less in diameter (airspace or acinar nodules) and poorly defined centrilobular nodules are frequently associated (Fig. 1) .[17]

Figure 1. Bronchopneumonia in a 20-year-old man. Thin-section (1-mm collimation) CT scan obtained at level of suprahepatic inferior vena cava shows centrilobular nodules and branching linear structures *(straight arrows)*, acinar nodules of 4 to 10 mm in diameter *(curved arrows)*, and lobular consolidation *(arrowheads)* of 10 to 20 mm in diameter in both lungs.

Because alveolar filling disorders include various diseases with overlapping CT findings, it is difficult to distinguish among the alveolar filling disorders with CT findings alone. Integration of HRCT findings, including disease pattern and distribution, and time factors including both evolution and resolution of the disease, however, may enable a narrower differential diagnosis of alveolar filling diseases (Table 1) . In this article, the authors review the most important and common alveolar filling disorders, focusing on pathologic and HRCT findings.

TABLE 1 -- HELPFUL HIGH-RESOLUTION CT AND TIME FACTORS IN DIFFERENTIATING

ALVEOLAR FILLING DISEASES
HRCT Findings
Widely disseminated
PCP, CMV pneumonia, acute PE, ARDS, DPH, PAP, BAC, BOOP, CEP, and CSS
Localized
Segmental or peribronchial: pneumonia with *S. aureus* and *St. pyogenes*, gram-negative organisms, lipoid pneumonia, pulmonary infarction
Nonsegmental: pneumonia with *St. pneumoniae*, *K. pneumoniae*, *Legionella* species, *M. tuberculosis*, radiation pneumonitis, BAC, and BALT lymphoma
Time Factors
Acute (within 2 weeks)
Actue pneumonia, PE, ARDS, DPH, and pulmonary infarction
Subacute or chronic (more than 1 month)
Chronic pneumonia (actinomycosis, semi-invasive pulmonary aspergillosis, TB, histoplasmosis), radiation pneumonitis, PAP, lipoid pneumonia, BAC, BOOP, CEP, CSS, and BALT lymphoma
PCP = *Pneumocystic carinii* pneumonia; CMV = cytomegalovirus; PE = pulmonary edema; ARDS = adult respiratory distress syndrome; BOOP = bronchiolitis obliterans organizing pneumonia; DPH = diffuse pulmonary hemorrhage; BAC = bronchioloalveolar carcinoma; TB = tuberculosis; PAP = **pulmonary alveolar proteinosis**; CEP = chronic eosinophilic pneumonia; CSS = Churg-Strauss syndrome; BALT = bronchus-associated lymphoid tissue.

SPECIFIC DISEASES

Pneumonia

Acute Pneumonia

Community-Acquired Pneumonia.

This is one of the most frequent causes of acute alveolar filling disorders. Radiologic and pathologic findings vary by types of pneumonia, namely bacterial pneumonia and atypical pneumonia. Bacterial pneumonia, especially pneumonia induced by gram-positive organisms, creates an inflammatory response in the peripheral lung and produces an outpouring of edema fluid that rapidly spreads to the adjacent acini, lobules, segments, and a lobe (Fig. 2) . These rapidly progressing changes cause relatively large consolidative lesions (the same size or larger than acinar nodules) on CT. Smaller shadows, such as centrilobular nodules and branching linear structures (tree-in-bud), are significantly fewer, and ground-glass opacity, which indicates incomplete filling of alveoli, is seen only around airspace consolidation. In contrast, patients with atypical pneumonia usually have smaller lesions such as centrilobular and acinar nodules and airspace consolidation of lobular size. These lesions are associated with

ground-glass opacity (partial filling of alveolar spaces with exudates consisting of fluid, cellular debris, and organisms). These abnormalities tend to be distributed fairly uniformly at the inner zone and at the middle and outer zones.[43]

Figure 2. Klebsiella pneumonia in a 44-year-old man. Enhanced CT (7-mm collimation) scan obtained at level of right upper lobar bronchus shows lobar consolidation in right upper lobe. Lobar volume is maintained. Also note patent bronchi within the lobar consolidation.

Pneumocystis Carinii Pneumonia.

The typical case of this infection is characterized histologically by alveolar and interstitial inflammation, proliferation of type II alveolar epithelial cells, and eosinophilic exudate within alveolar airspaces. Other histologic findings that may be seen either alone or in association with the typical features include diffuse alveolar damage, granulomatous inflammation, bronchiolitis obliterans organizing pneumonia, vascular invasion, vasculitis, parenchymal calcification, necrosis, and cyst formation.[44]

In the early stage of disease, scattered foci of ground-glass opacity (Fig. 3) or airspace consolidation (Fig. 4) can be seen on HRCT, corresponding histologically to areas of intra-alveolar exudates and some degree of thickening of the alveolar septa. With time, reticular opacities and intralobular linear opacities can be seen in association with ground-glass opacity. Reticular opacities reflect organization of intra-alveolar exudates with resultant thickening of the pulmonary interstitium. Following therapy, residual change such as parenchymal irregular linear opacities, peripheral bronchiectasis, and bronchiolectasis can be seen on CT. Cystic changes are identified on CT with a prevalence of about 10% to 34%.[6]

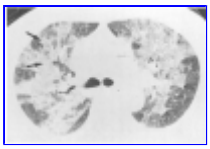

Figure 3. *Pneumocystis carinii* pneumonia in a 60-year-old woman with rheumatoid arthritis who had steroid therapy. Thin-section (1-mm collimation) CT scan obtained at level of right upper lobar bronchus shows patchy ground-glass opacity in both lungs. Also note areas of intralobular smooth linear opacities *(arrows)* in right upper lobe.

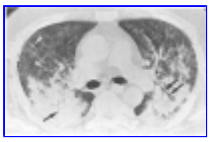

Figure 4. *Pneumocystis carinii* pneumonia in a 40-year-old man who underwent chemotherapy for anaplastic astrocytoma. Thin-section (1-mm collimation) CT scan obtained at subcarinal level showed patchy airspace consolidation with air-bronchograms *(arrows)*. Note some ground-glass opacity and small nodules *(arrowheads)*.

Cytomegalovirus Pneumonia.

Cytomegalovirus pneumonia may lead to an interstitial pneumonia, inflammatory or hemorrhagic nodules, and in severe cases, diffuse alveolar damage. Histologic findings include mononuclear interstitial infiltrates, thickened interlobular septa, and diffuse alveolar damage consisting of fibrinous exudate, hemorrhage, and hyaline membrane formation.[35] Lung involvement is most commonly diffuse, but it may be nodular or confined to a single lobe.

Depending on the severity, distribution, and relative proportions of alveolar filling (diffuse alveolar damage including intra-alveolar hemorrhage) and interstitial thickening (lymphocytic infiltration and thickening of alveolar wall and interlobular septa), HRCT may show ground-glass opacity, dense consolidation, mass-like infiltrates, poorly defined centrilobular nodules, irregular linear opacity, or any combination of these (Fig. 5).[1] [35] [37] Moon et al[37] described the HRCT findings of cytomegalovirus (CMV) pneumonia in non-AIDS immunocompromised patients. They were bilateral mixed areas of ground-glass opacity, poorly defined centrilobular small nodules, and consolidation. Interlobular septal thickening and pleural effusion are associated frequently.

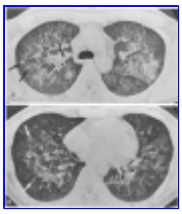

Figure 5. Cytomegalovirus pneumonia in a 26-year-old man who underwent bone marrow transplantation because of aplastic anemia. Thin-section (1-mm collimation) CT scans obtained at levels of azygos arch *(A)* and right atrium *(B)*, respectively, show diffuse bilateral ground-glass opacity, patchy airspace consolidation, and some poorly defined centrilobular nodules *(arrows)*.

Chronic Pneumonia

Actinomycosis.

Thoracic actinomycosis usually is caused by aspiration of infected material in the oropharynx. Pulmonary involvement has been reported to be most common in alcoholic persons. The presence of chronic pneumonia, chronic pleural effusion, and periosteal rib involvement, usually accepted as a diagnostic triad, has been described as a well-recognized mode of presentation.[15]

Histologically, actinomycotic abscess is composed of an outer rim of granulation tissue and inner masses of polymorphonuclear leukocytes that contain typical actinomycotic or sulfur granules. Actinomycotic or sulfur granules are round or oval slightly lobulated basophilic masses. In the center of the granules, organisms are identified as gram-positive or Gomori-methenamine-silver stain–positive filaments. Sometimes dilated bronchi that contain actinomycotic granules are seen within the areas of consolidation.

According to a recent report by Cheon et al,[9] the typical CT findings of thoracic actinomycosis are chronic airspace consolidation that contain low-attenuation areas (representing actinomycotic or sulfur granules) with peripheral enhancement (representing granulation tissue in the wall of abscess) and adjacent pleural thickening. Airspace consolidation usually is segmental in distribution (Fig. 6) .

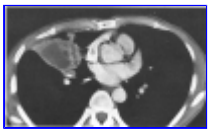

Figure 6. Actinomycosis in a 40-year-old man. Enhanced CT (7-mm collimation) scan obtained at left atrial level shows airspace consolidation in right middle lobe containing large central necrotic area with low attenuation. A necrotic low-attenuation area is conspicuous, contrasted with surrounding parenchymal enhancement.

Semi-Invasive Pulmonary Aspergillosis.

Semi-invasive pulmonary aspergillosis (pathologically described as chronic necrotizing pulmonary aspergillosis) is defined as an indolent infiltrative process caused by a fungus of the *Aspergillus* species. In patients with semi-invasive pulmonary aspergillosis, abnormalities in the host's defense mechanism are frequently present. Typically, patients have poor nutrition caused by alcoholism, diabetes, chronic granulomatous disease, or connective tissue disorders. Patients may have undergone low-dose corticosteroid therapy. Pulmonary abnormalities such as a fibrotic area caused by *Mycobacterium* species, chronic obstructive lung disease, previous surgery, radiation therapy, pulmonary infarction, or pneumoconiosis may lower further the pulmonary defense mechanisms.[27] Yousem[47] reported three morphologic patterns of chronic necrotizing pulmonary aspergillosis: a necrotizing granulomatous pneumonia, a granulomatous bronchiectatic cavity with parenchymal invasion, and a bronchocentric granulomatosis-like reaction.

CT findings of semi-invasive pulmonary aspergillosis are diverse. They include areas of lobar or segmental consolidation and a low-attenuation mass[27] (Fig. 7) . Saprophytic aspergillosis (mycetomas) develops in immunologically normal patients with lungs that are structurally abnormal caused by cavitary disease of prior tuberculosis or sarcoidosis.

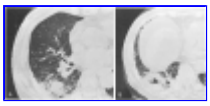

Figure 7. Semi-invasive pulmonary aspergillosis in a 75-year-old woman with chronic renal failure. Thin-section (1-mm collimation) CT scans obtained at levels of right middle lobar bronchus *(A)* and liver dome *(B)*, respectively, show round areas of airspace consolidation containing cavitation and dilated bronchi in right lower lobe. Also note underlying pulmonary fibrosis with honeycombing and irregular linear opacities.

Histoplasmosis.

Pulmonary histoplasmosis appears in two forms: acute and chronic. Acute pulmonary histoplasmosis results in poorly defined nonsegmental opacity. Chronic cavitary histoplasmosis always is associated with chronic obstructive pulmonary disease. The disease is similar in appearance to postprimary tuberculosis. Affected patients have progressive, predominantly upper lobe disease characterized by fibrosis, necrosis, cavitation, and granulomatous inflammation.[41]

The radiologic appearances in chronic cavitary histoplasmosis simulate postprimary tuberculosis; the earliest manifestations consisted of segmental or nonsegmental areas of consolidation in the apices of the lungs, frequently outlining spaces of centrilobular emphysema.[41]

Pulmonary Edema

Although hydrostatic (cardiogenic) and permeability (noncardiogenic) edema with or without diffuse alveolar damage cannot be distinguished on the basis of CT findings alone; their appearances tend to differ. Hydrostatic edema results generally in a combination of septal thickening and ground-glass opacity.[42] Thickening of the parahilar peribronchovascular interstitium (peribronchial cuffing) and fissures also are common.[16] Haze poorly defined centrilobular opacities also are seen.[20] There is a tendency for hydrostatic edema to have a perihilar and gravitational distribution.

Adult respiratory distress syndrome (ARDS) is the term used for various acute or subacute diffuse pulmonary lesions that cause severe hypoxemia.[5] These lesions are associated with a variety of precipitating factors and are not caused or influenced by concurrent cardiac insufficiency. ARDS represent the most severe form of permeability edema associated with diffuse alveolar damage. The distribution of CT abnormalities in ARDS are bilateral (92%), gravity-dependent (86%), and at the bases (68%) of the lungs. CT shows homogeneous appearance in only a quarter of the cases; the rest show either patchy consolidation (42%) or mixed airspace consolidation and ground-glass opacity (Fig. 8) . The vast majority of the cases have air bronchograms (89%). Approximately one half of the cases have pleural effusions, either bilateral (28%), or unilateral (22%), and in the majority of cases, the amount is small. On the basis of etiologic differences, two major pathophysiologic mechanisms in the development of ARDS have been described: ARDS caused by an underlying pulmonary disease and ARDS caused by an extrapulmonary disease. ARDS caused by pulmonary disease tends to be asymmetric with a mix of consolidation and ground-glass opacity, whereas ARDS caused by extrapulmonary disease has predominantly symmetric ground-glass opacity. In both groups, pleural effusion and air bronchograms are common, and Kerley B lines and pneumatoceles are uncommon.[19]

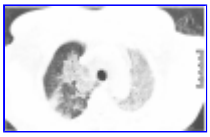

Figure 8. Adult respiratory distress syndrome in a 91-year-old woman. Thin-section (1-mm collimation) CT scan obtained at level of aortic arch shows patchy ground-glass opacity in both upper lobes.

Acute interstitial pneumonia (AIP) is a fulminant disease of unknown cause that produces histologic hallmark of diffuse alveolar damage. Diffuse alveolar damage observed in AIP is identical to the alveolar damage in ARDS; however, no cause is identifiable. AIP may be considered an idiopathic ARDS.[38] Recently, Ichikado et al[22] evaluated the relation between pathologic phases of AIP and HRCT findings in 17 biopsy sites from 14 patients. They found that areas of increased attenuation without traction bronchiectasis were associated with either exudative or early proliferative phase (Fig. 9) . Areas of increased attenuation with traction bronchiectasis were associated with either proliferative or fibrotic phase. Areas of honeycombing corresponded to restructuring of distal airspaces

and dense interstitial fibrosis. They concluded that the findings of traction bronchiectasis in areas of increased attenuation at least suggest the proliferative or fibrotic phase of AIP.

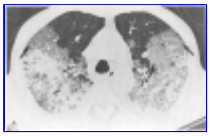

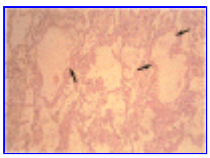

Figure 9. Acute interstitial pneumonia in a 63-year-old man. *A*, Thin-section (1-mm collimation) CT scan obtained at level of azygos arch shows extensive ground-glass opacity and patchy consolidation with interlobular septal thickening *(arrows)*. *B*, See Color Plate on p 1219.

Radiation Pneumonitis and Fibrosis

Radiation pneumonitis refers to the acute lung changes that occur approximately 8 weeks after completion of radiation therapy of 40 Gy or more of radiation dose. It may appear somewhat earlier when higher doses of radiation are applied.[13] The earliest radiographic changes in radiation pneumonitis may be subtle with slight indistinctness around vessels and faint hazy opacity, or they may be more marked with patchy or homogeneous airspace consolidation. Although these radiographic findings may resolve completely, progression to fibrosis usually occurs, particularly when the acute changes are severe.[13]

CT is more sensitive than chest radiography for showing radiation effects. In one study of 17 patients examined with serial CT scans performed after completion of radiation therapy, abnormalities were visible on CT scans within 4 weeks in 13 patients and within 16 weeks in 15.[23] Libshitz and Shuman[33] described four CT patterns of radiation pneumonitis: (1) homogeneous, slight increase in attenuation, uniformly involving the irradiated portion of lung (Fig. 10) (Figure Not Available) ; (2) patchy consolidation within the irradiated lung, not necessarily conforming to the shape of the portal; (3) discrete consolidation, conforming to the shape of the portal, but not uniformly outlining it; and (4) solid consolidation, conforming to and totally involving the irradiated region of lung. The lung opacities evolve over time after completion of radiation therapy, beginning with slightly increased opacity, progressing to patchy opacities, and later to discrete and solid consolidation. This progression reflects the transition from pneumonitis to fibrosis. In many patients, a straight border corresponding to the radiation port is evident between the irradiated, opacified lung and the healthy lung. Findings within the radiation portal are not always uniform. The inhomogeneity of radiation pneumonitis may reflect variations in dose to different parts of the lung.

Figure 10. (Figure Not Available) Acute lung injury after limited thoracic irradiation in a 61-year-old man who underwent left upper lobectomy caused by lung cancer. *A*, Thin-section (1-mm collimation) CT scan obtained at subcarinal level shows diffuse bilateral ground-glass opacity in both lungs. Also note consolidation *(large arrow)* in posterior segment of right upper lobe and traction bronchiectasis *(small arrows)* in right upper lobe. Intralobular smooth linear opacities (crazy paving) *(arrowheads)* are seen in left lower lobe. A gas collection is seen anteriorly in left upper lobectomy space. *B*, See Color Plate on p 1219.*(From Hwang JH, Lee KS, Song KS, et al: Extensive acute lung injury following limited thoracic irradiation: Radiologic findings in three patients. J Korean Med Sci 15:697–702, 2000; with permission.)*

Limited thoracic irradiation results occasionally in acute lung injury. In this condition, chest radiograph shows diffuse ground-glass appearance in both lungs and thin-section CT scans show diffuse bilateral ground-glass opacity with traction bronchiectasis, interlobular septal thickening, and intralobular smooth linear opacities. In these occasions, pathology shows diffuse alveolar damage (Fig. 10) (Figure Not Available) . [21]

Figure 10. (Figure Not Available) Acute lung injury after limited thoracic irradiation in a 61-year-old man who underwent left upper lobectomy caused by lung cancer. *A*, See p 1218. *B*, High-magnification (H & E, original magnification ×200) photomicrograph of open lung biopsy specimen obtained from right middle lobe shows interstitial fibroblastic accumulation *(arrows)* with hyperplasia of type II pneumocytes *(arrowheads).(From Hwang JH, Lee KS, Song KS, et al: Extensive acute lung injury following limited thoracic irradiation: Radiologic findings in three patients. J Korean Med Sci 15:697–702, 2000; with permission.)*

Unusual treatment ports also are well delineated on CT. For example, the tangential-beam technique, used in the treatment of breast carcinoma, results in a characteristic CT appearance, with parenchymal opacities confined to the anterolateral subpleural region of lung.[12]

Pulmonary Alveolar Proteinosis

Pulmonary alveolar proteinosis is a disease characterized by filling of the alveolar airspaces with periodic-acid–Schiff–positive proteinaceous materials. The pathogenesis of this disease is understood poorly, but may be seen in one of four clinical settings: as an idiopathic disease, as an occupational disease, as a drug-induced disease, and an infiltrate in the immunocompromised host. The occupational cause is the most common result associated with exposure to silica, although other substances also have been implicated experimentally and clinically.[36] Lesions resembling proteinosis have been discussed in relation to amphophilic drugs. In the immunocompromised host, the underlying diseases usually are leukemia or lymphoma, and most of these patients have been treated with busulphan.[40]

Pulmonary alveolar proteinosis is more common in men than in women by a ratio 4 to 1. Patients range in age from a few months to more than 70 years, with two thirds of patients between 30 and 50 years old.[18] Symptoms usually are mild and of insidious onset. They include nonproductive cough, fever, and mild dyspnea on exertion. Although plain radiographs often are strikingly abnormal, patients may complain of only a mild degree of respiratory impairment. The radiographic abnormality consists of widespread airspace opacification or confluent poorly defined (acinar) nodules in a bilateral, central, or basal distribution, resembling pulmonary edema.[18]

The combination of a geographic distribution of areas of ground-glass opacity and smoothly thickened interlobular septa within the areas of airspace disease, resulting in “crazy-paving” appearance, is strongly suggestive of **alveolar proteinosis** on CT (Fig. 11) . Air bronchograms surprisingly are uncommon. Thickening of the interlobular septum is probably caused by septal edema. Ground-glass opacity results from filling of alveolar spaces with periodic-acid–Schiff–positive proteinaceous materials. There also may be infiltration of alveolar walls by lymphocytes, macrophages, and edema fluid, which is likely the cause of the intralobular interstitial thickening visible on HRCT. Because this interstitial thickening may resolve after treatment with bronchoalveolar lavage, it can be presumed to represent edema or cellular infiltration rather than fibrosis in most cases.[18]

Figure 11. Pulmonary alveolar proteinosis in a 42-year-old man. Targeted image of thin-section (1.5-mm collimation) CT scan obtained at level of liver dome shows patchy areas of ground-glass opacity with intralobular smooth linear opacities (crazy paving) in right lung.

CT can also demonstrate focal pneumonia in patients with the disease that is not apparent on chest radiographs. By detecting focal areas of dense consolidation or abscess formation, CT may confirm a clinical suspicion of superimposed infection (particularly *Nocardia asteroides* infection).[18]

The crazy-paving pattern on HRCT may be a nonspecific finding. The principal differential diagnostic considerations for the crazy-paving appearance include mucinous bronchioloalveolar carcinoma, exogenous lipoid pneumonia, pulmonary edema, *Pneumocystis carinii* pneumonia, adult respiratory distress syndrome, radiation pneumonitis, drug_induced pneumonitis, and pulmonary hemorrhage.[26]

Lipold Pneumonia

The pathology of exogenous lipoid pneumonia with chronic aspiration or inhalation of mineral, vegetable, and animal oil is a simple foreign body reaction in the lung. Patients at particular risk of exogenous lipoid pneumonia include neonates, older patients, and those with any underlying swallowing dysfunction such as achalasia, esophageal diverticulum, hiatal hernia, and neuromuscular disorders of the pharynx and esophagus.[31]

Early in oil aspiration pneumonia, parenchymal abnormalities consist of localized or widespread areas of alveolar consolidation. Lipid-laden macrophages increase in number in the alveoli, are incorporated into the alveolar walls, and may reach the interlobular septa through the lymphatics. The alveolar walls and interlobular septa become thickened by reticulin fibers and are infiltrated with lymphocytes and plasma cells. Repeated aspiration may lead to proliferative fibrotic pneumonitis and may result rarely in severe fibrosis and cor pulmonale.[7]

The diagnosis of disease is confirmed by a clinical history of ingestion or inhalation of the oily material or by seeing the lipid-laden macrophages in bronchoalveolar lavage fluid or on transbronchial biopsy specimens.[31]

Chest radiographic findings of lipoid pneumonia are nonspecific and consist of ground-glass opacity, consolidation, and poorly defined nodules.[31] The most frequent parenchymal abnormalities on CT scans consist of bilateral areas of ground-glass opacity, poorly defined centrilobular nodules, crazy paving, and consolidation. The abnormalities are distributed in the right middle lobe, lingular segment of the left upper lobe, and in both lower lobes (Figs. 12 and 13).[31] The CT attenuation of the parenchymal consolidation at mediastinal window settings, which reflects pathologically the mixture of fat and inflammatory reaction, is slightly higher than that of subcutaneous fat and lower than that of chest wall muscle.[32] Follow-up CT scans demonstrate decrease or no change because the lesions are indolent and remain after cessation of ingestion.

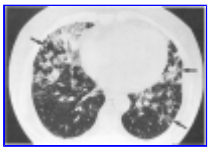

Figure 12. Squalene-induced extrinsic lipoid pneumonia in a 45-year-old woman. Thin-section (1-mm collimation) CT scan obtained at level of right inferior pulmonary vein shows patchy areas of ground-glass opacity in right middle lobe and in lingular segment of left upper lobe. Also note poorly defined centrilobular nodules *(arrows)* in both lungs.

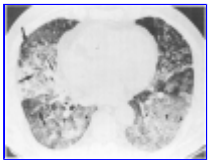

Figure 13. Squalene-induced extrinsic lipoid pneumonia in a 63-year-old man with idiopathic thrombocytopenic purpura. Thin-section (1-mm collimation) CT scan obtained at level of basal segmental bronchi shows diffuse areas of ground-glass opacity and some poorly defined centrilobular nodules *(arrows)* in both lungs. Also note intralobular smooth linear opacities *(arrowheads)* in ground-glass opacity.

Pulmonary Hemorrhage

Diffuse pulmonary hemorrhage is characterized by widespread parenchymal hemorrhage from the microvasculature of the lung and occurs in a large group of disorders. The disorders have overlapping features of glomerulonephritis, immune complex, and antiglomerular basement membrane disease.[2] In idiopathic pulmonary hemosiderosis, neither renal disease nor immunologic association is demonstrable. Other miscellaneous causes of pulmonary hemorrhage include drugs and bleeding diatheses.[8] The clinical features include recurrent hemoptysis, chronic cough, dyspnea, and an iron deficiency anemia.

Acute pulmonary hemorrhage appears as areas of ground-glass opacity or sometimes as frank consolidation on HRCT (Fig. 14 and 15). These abnormalities usually resolve rapidly during remission. Discrete pulmonary nodules of uniform size are identifiable in patients whose CT scans are obtained during complete or partial clinical remission. Focal accumulation of hemosiderin and hemosiderin-laden macrophages within alveoli may give a nodular appearance on HRCT.[8] The conspicuity of the smaller nodules probably is caused by the high-molecular-weight hemosiderin components that contribute to an increase in CT attenuation.

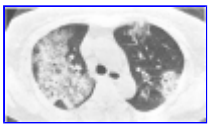

Figure 14. Pulmonary hemorrhage in a 60-year-old woman with Wegener's granulomatosis. Thin-section (1-mm collimation) CT scan obtained at level of aortopulmonary window shows multifocal patchy areas of ground-glass opacity plus airspace consolidation. Pulmonary hemorrhage was confirmed with bronchoalveolar lavage.

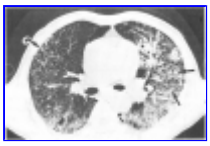

Figure 15. Hemorrhagic pneumonitis in a 63-year-old man with leptospirosis. Thin-section (1-mm collimation) CT scan obtained at subcarinal level shows patchy areas of ground-glass opacity plus consolidation in both lungs. Also note poorly defined small nodules *(arrows)* in both lungs.

Bronchioloalveolar Carcinoma

Bronchioloalveolar carcinoma is characterized pathologically by lepidic growth with preservation of lung architecture. The most frequent symptoms and signs in patients with bronchioloalveolar carcinoma include cough, sputum, shortness of breath, weight loss, hemoptysis, and fever. Bronchorrhea, once considered the clinical hallmark of this disease, is unusual and a late manifestation seen only with diffuse bronchioloalveolar carcinoma.[11] [34]

The radiologic manifestations of bronchioloalveolar carcinoma are diverse and include single or multiple pulmonary nodules, segmental or lobar consolidation, and diffuse airspace disease (Fig. 16) . Alveolar filling disorders usually are seen in forms of segmental or lobar and diffuse airspace disease. The lobar consolidative form accounts for approximately 30% of all bronchioloalveolar carcinomas and corresponds to a mucinous histologic type. The airspace consolidation is caused by growth along the alveolar wall combined with secretion of mucin. Production of copious amounts of mucin may result in expansion of the involved lobe, leading to bulging of interlobar fissures.

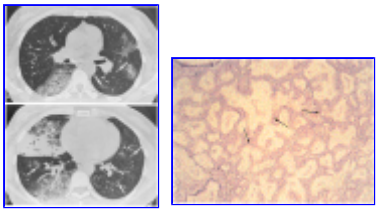

Figure 16. Bronchioloalveolar carcinoma of diffuse type in a 45-year-old woman. *A*, Thin-section (1-mm collimation) CT scan obtained at level of bronchus intermedius shows patchy ground-glass opacity in both lungs. Also note poorly defined centrilobular nodules *(arrows). B*, CT scan obtained at level of inferior pulmonary vein shows segmental airspace consolidation with air-bronchograms and air-bronchiolograms in right middle lobe. Also note patchy areas of ground-glass opacity and poorly defined centrilobular nodules *(arrows)* in both lungs. *C*, See Color Plate on p 1219.

The CT angiogram sign is caused by the homogeneous low attenuation of consolidation, which allows vessels to be seen clearly particularly after intravenous administration of contrast material. The CT angiogram sign is nonspecific and also may be seen in lobar pneumonia, pulmonary lymphoma, extrinsic lipid pneumonia, pulmonary infarction, and pulmonary edema. According to a recent report by Arika et al,[3] diffuse bronchioloalveolar carcinoma can be classified into three patterns: ground-glass opacity (the most common) consolidation, and multiple nodules. Areas of ground-glass opacity are found both around and remote from the consolidation or nodule.

Chronic Eosinophilic Pneumonia

Chronic eosinophilic pneumonia is characterized pathologically by eosinophilic and lymphocytic accumulation in the alveoli and interstitium. Interstitial fibrosis and eosinophilic abscess may be seen. Histologic features of bronchiolitis obliterans organizing pneumonia or low-grade vasculitis also may be present.[28]

The symptoms are insidious and continue for at least 1 month before diagnosis in all patients. They include cough, fever, dyspnea, and weight loss. Peak incidence of the disease is in the fifth decade. Forty percent of patients have associated asthma. Women are involved more frequently than men (2 to 1 ratio).

Chest radiograph classically shows bilateral areas of nonsegmental consolidation in a subpleural distribution. This pattern is seen in 60% of cases. Nodules with or without cavitation are present in 20% of cases. Pleural effusions are rare and observed in less than 10% of patients.[25] CT scan also shows subpleural areas of consolidation; this demonstrates peripheral dominance more clearly and frequently than chest radiograph. In the early stage of the disease, consolidation is the predominant abnormality on CT, whereas nodules or reticular densities predominate in later stages (Fig. 17) .[14]

Figure 17. Chronic eosinophillic pneumonia in a 27-year-old man. Thin-section (1-mm collimation) CT scan obtained

at level of bronchus intermedius shows multifocal patchy areas of consolidation and ground-glass opacity in the subpleural area of both lungs.

Churg-Strauss Syndrome (Allergic Angiitis and Granulomatosis)

Churg-Strauss syndrome is characterized by hypereosinophilia and systemic vasculitis occurring in patients with asthma and allergic rhinitis. There are three major histologic criteria in the diagnosis of the disease: necrotizing vasculitis, tissue infiltration by eosinophils, and extravascular granulomas.[28] Multiple organs involved are upper airways, lung, skin, nerve, gastrointestinal tract, heart, kidneys, and joints. Upper airway disease and pulmonary abnormalities are most common and occur in approximately 70% of patients.[29] Asthma and peripheral eosinophilia antedate the systemic vasculitis in approximately 40% of patients.

Chest radiograph demonstrates transient, patchy, nonsegmental consolidation; however, small noncavitary nodules or diffuse reticular opacities also have been reported. Pleural effusion occurs in 30% of the patients, and hilar lymph node enlargement has been reported occasionally. In one study of nine patients with Churg-Strauss syndrome,[10] most frequent HRCT findings were areas of ground-glass opacity (100%), centrilobular micronodules in areas of ground-glass opacity (89%), or consolidation (56%), distributed at the subpleural lower lung zone. Associated findings were bronchial wall thickening (78%), macronodules (44%), interlobular septal thickening (22%), pleural effusion (22%), and pericardial effusion (22%) (Fig. 18) .

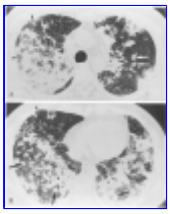

Figure 18. Churg-Strauss syndrome in a 28-year-old man with asthma. Thin-section (1-mm collimation) CT scans obtained at levels of distal trachea *(A)* and inferior vena cava *(B)*, respectively, show multifocal patchy areas of airspace consolidation, ground-glass opacity, acinar nodules *(arrows)*, and poorly defined centrilobular nodules and branching linear structures *(arrowheads)*.

Drug-Induced Lung Disease

The histopathologic manifestations of drug-induced lung disease are diverse and include patterns of diffuse alveolar damage, bronchiolitis obliterans organizing pneumonia, eosinophilic pneumonia, obliterative bronchiolitis, and pulmonary edema and hemorrhage. Except for a pattern of obliterative bronchiolitis, the remaining four patterns show alveolar filling disorders. Because the clinical and imaging findings of drug-induced lung disease generally reflect the underlying histopathologic process, it is important to be aware of which drugs cause which pattern of histopathology.

Bronchus-Associated Lymphoid Tissue Lymphoma

Primary lymphomas of the lung are exceedingly rare tumors, accounting 0.4% to 1% of all lymphomas. Up to 70% of primary lymphomas of the lung are bronchus-associated lymphoid tissue (BALT) lymphomas (arising from the mucosa-associated lymphoid tissue).The majority of primary pulmonary lymphomas are low-grade, B-cell, non-Hodgkin's lymphomas that show a good prognosis.[38] [46]

Histologically, low-grade BALT lymphomas are composed of centrocyte-like, lymphocyte-like, or monocytoid cells that derive from the marginal zone of the BALT structures. Colonization of germinal centers and lymphoepithelial lesions is typical. The pattern of infiltration is along bronchovascular bundles and interlobular septa, suggesting that the spread of disease is along the lymphatic axis.[46]

The most common radiographic abnormalities consist of solitary or multiple pulmonary nodules or multiple areas of patchy consolidation. Hilar and mediastinal lymphadenopathy is very rare. In one study of BALT lymphoma in 10 patients, BALT lymphomas usually appear as airspace consolidation (60%) or nodules (60%) with air bronchograms (90%) or adjacent ground-glass attenuation (70%) at CT (Fig. 19) . Multiplicity of disease was seen in seven

patients and bilateral lung lesions in six. Bubble-like radiolucencies (50%) have not been described previously and can be an additional finding of BALT lymphoma.[30]

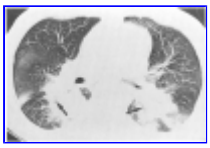

Figure 19. Bronchus-associated lymphoid tissue lymphoma in a 60-year-old man. Thin-section (1-mm collimation) CT scan obtained at level of bronchus intermedius shows consolidation in superior segments of both lower lobes. Air bronchograms *(arrows)* are seen in consolidation. (Courtesy of Nestor L Müller, MD, PhD, Vancouver, BC, Canada.)

Pulmonary Infarction

Pulmonary infarction presents characteristically as pleural based focal masses with convex bulging lateral border (representing Hampton's hump) and linear strands directing from the apex of the lesion toward the pulmonary hilus and scattered areas of low attenuation within the lesion (Fig. 20) . This distinctive complex of findings on CT should raise a strong suspicion of pulmonary infarction. An apparent feeding vessel also may be identified. On CT scan, peripheral enhancement is seen frequently along the margins of the infarct including the pleural surfaces; presumably this is the result of collateral perfusion from the bronchial arterial circulation.[4]

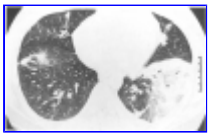

Figure 20. Pulmonary infarct in a 28-year-old man with pulmonary thromboembolism. Thin-section (1-mm collimation) CT scan obtained at ventricular level shows segmental consolidation and ground-glass opacity in left lower lobe. Also note poorly defined nodules in right lung and left upper lobe.

SUMMARY

Airspace filling process is characterized on CT by the presence of one or more fairly homogeneous areas of consolidation with little or no volume loss. The consolidation may be segmental, subsegmental, lobular, or acinar (10 mm or less in diameter). Poorly defined centrilobular nodules may be associated. The margin of the consolidation usually is poorly defined except in the areas in which the consolidation abuts the pleura. Air-containing bronchi or bronchioles (CT air bronchograms or air bronchiolograms) are seen frequently. Many diseases can present with alveolar filling disorders. Because the HRCT findings overlap among various alveolar filling disorders, it may be impossible to make a definite diagnosis with HRCT findings alone. Integration of HRCT findings including disease pattern and distribution and time factors including evolution and resolution of the disease, however, may enable to narrow differential diagnosis of alveolar filling diseases. Furthermore, clinical and laboratory findings also may provide helpful clues to reach a reasonable diagnosis. The role of HRCT in alveolar filling disorders is not limited to diagnosis. HRCT also plays a useful role in determining the extent of disease and in identifying accompanying abnormalities, and complications of the primary disease.

References

1. Aafedt BC, Halvorsen RA, Tylen U, et al: Cytomegalovirus pneumonia: Computed tomography findings. J Can Assoc Radiol 41:276–280, 1990

2. Albelda SM, Gefter WB, Epstein DM, et al: Diffuse pulmonary hemorrhage: A review and classification. Radiology 154:289–297, 1985 Abstract

3. Arika M, Atagi S, Kawahara M, et al: High-resolution CT findings of diffuse bronchioloalveolar carcinoma in 38 patients. AJR Am J Roentgenol 173:1623–1629, 1999 Abstract

4. Balakrishnan J, Meziane MA, Siegelman SS, et al: Pulmonary infarction: CT appearance with pathologic correlation. J Comput Assist Tomogr 13:941–945, 1989 Abstract

5. Bernard GR, Artigas A, Brigham KL, et al: The American-European Consensus Conference on ARDS. Definitions, mechanisms, relevant outcomes, and clinical trial coordination. Am J Respir Crit Care Med 149:818–824, 1994. Abstract

6. Boiselle PM, Crans CA, Kaplan MA: The changing face of pneumocystis carinii pneumonia in AIDS patients. AJR Am J Roentgenol 172:1301–1309, 1999 Abstract

7. Casey JF: Chronic cor pulmonale associated with lipoid pneumonia. JAMA 76:896–898, 1961

8. Cheah FK, Sheppard MN, Hansell DM: Computed tomography of diffuse pulmonary hemorrhage with pathologic correlation. Clin Radiol 48:89–93, 1993 Abstract

9. Cheon JE, Im JG, Kim MY, et al: Thoracic actinomycosis: CT findings. Radiology 209:229–233, 1998 Abstract

10. Choi YH, Im JG, Han BK, et al: Thoracic manifestation of Churg-Strauss syndrome: Radiologic and clinical findings. Chest 117:117–124, 2000 Full Text

11. Clayton F: Bronchioloalveolar carcinomas: Cell types, patterns of growth, and prognostic correlates. Cancer 57:1555–1564, 1986 Abstract

12. Coscina WF, Arger PH, Mintz MC, et al: CT demonstration of pulmonary effects of tangential beam radiation. J Comput Assist Tomogr 10:600–602, 1986 Abstract

13. Davis SD, Yankelevitz DF, Henschke CI. Radiation effects on the lung: Clinical features, pathology, and imaging findings. AJR Am J Roentgenol 159:1157–1164, 1992 Citation

14. Ebara H, Ikezoe J, Johkoh T, et al: Chronic eosinophilic pneumonia: Evolution of chest radiograms and CT features. J Comput Assist Tomogr 18:737–744, 1994 Abstract

15. Flynn MW, Felson B. The roentgen manifestations of thoracic actinomycosis. AJR Am J Roentgenol 10:707–716, 1970

16. Forster BB, Müller NL, Mayo JR, et al: High-resolution computed tomography of experimental hydrostatic pulmonary edema. Chest 101:1434–1437, 1992 Abstract

17. Gamsu G, Thurlbeck WM, Macklem PT, et al: Roentgenographic appearance of the human pulmonary acinus. Invest Radiol 6:171–175, 1971 Citation

18. Godwin JD, Müller NL, Takasugl JE: **Pulmonary alveolar proteinosis**: CT findings. Radiology 169:609–613, 1988 Abstract

19. Goodman LR, Fumagalli R, Tagliabue P, et al: Adult respiratory distress syndrome due to pulmonary and extrapulmonary causes: CT, clinical, and functional correlations. Radiology 213:545–552, 1999 Abstract

20. Gruden JF, Webb WR, Warnock M: Centrilobular opacities in the lung on high-resolution CT: Diagnostic considerations and pathologic

correlation. AJR Am J Roentgenol 162:569–574, 1994 Abstract

21. Hwang JH, Lee KS, Song KS, et al: Extensive acute lung injury following limited thoracic irradiation: Radiologic findings in three patients. J Korean Med Sci 15:697–702, 2000

22. Ichikado K, Johkoh T, Ikezoe J, et al: Acute interstitial pneumonia: High-resolution CT findings correlated with pathology. AJR Am J Roentgenol 168:333–338, 1997 Abstract

23. Ikezoe J, Takashima S, Morimoto S, et al: CT appearance of acute radiation-induced injury in the lung. AJR Am J Roentgenol 150:765–770, 1988 Abstract

24. Itoh H, Murata K, Konishi J, et al: Diffuse lung disease: Pathologic basis for the high-resolution computed tomography findings. J Thorac Imaging 8:176–188, 1993 Abstract

25. Jederlinic PJ, Sicilian L, Gaensler EA: Chronic eosinophilic pneumonia. A report of 19 cases and a review of the literature. Medicine 67:154–162, 1986

26. Johkoh T, Itoh H, Müller NL, et al: Crazy-paving appearance at thin-section CT: Spectrum of disease and pathologic findings. Radiology 211:155–160, 1999 Abstract

27. Kim SY, Lee KS, Han JH, et al: Semiinvasive aspergillosis: CT and pathologic findings in six patients. AJR Am J Roentgenol 174:795–798, 2000 Abstract

28. Kim Y, Lee KS, Choi DC: The spectrum of eosinophilic lung disease: Radiologic findings. J Comput Assist Tomogr 21:920–930, 1997 Abstract

29. Lanham JG, Elkon KB, Pusey CD, et al: Systemic vascularitis with asthma and esoniophilia: A clinical approach to the Churg-Strauss sundrome. Medicine 63:65–81, 1984 Abstract

30. Lee DK, Im JG, Lee KS, et al: B-cell lymphoma of bronchus-associated lymphoid tissue (BALT): CT features in 10 patients. J Comput Assist Tomogr 24:30–34, 2000 Abstract

31. Lee JY, Lee KS, Kim TS, et al: Squalene-induced extrinsic lipoid pneumonia: Serial radiologic findings in nine patients. J Comput Assist Tomogr 23:730–735, 1999 Abstract

32. Lee KS, Müller NL, Hale V: Lipoid pneumonia: CT findings. J Comput Assist Tomogr 19:48–51, 1995 Abstract

33. Libshitz HI, Shuman LS: Radiation-induced pulmonary changes: CT findings. J Comput Assist Tomogr 8:15–19, 1984 Abstract

34. Manning JT, Spjut HJ, Tschen JA: Bronchioloalveolar carcinoma: The significance of two histopathologic types. Cancer 54:525–534, 1984 Abstract

35. McGuinness G, Scholes JV, Garay SM, et al: Cytomegalovirus pneumonia: Spectrum of parenchymal CT findings with pathologic correlation in 21 AIDS patients. Radiology 192:451–459, 1994 Abstract

36. Miller RR, Churg AM, Hutcheon M, et al: **Pulmonary alveolar proteinosis** and aluminum dust exposure. Am Rev Respir Dis 130:312–315, 1984 Abstract

37. Moon JH, Kim EA, Lee KS, et al: Cytomegalovirus pneumonia: High-resolution CT findings in 10 non-AIDS immunocompromised patients. Korean J Radiol 1:73–78, 2000.

38. Ooi GC, Chim CS, Lie AK, et al: Computed tomography features of primary pulmonary non-Hodgkin's lymphoma. Clin Radiol 54:438–443, 1999 Abstract

39. Primack SL, Hartman TE, Ikezoe J, et al: Acute interstitial pneumonia: Radiographic and CT findings in nine patients. Radiology 188:817–820, 1993 Abstract

40. Ruben FL, Talamo TS: Secondary **pulmonary alveolar proteinosis** occurring in two patients with acquired immune deficiency syndrome. Am J Med 80:1187–1190, 1986 Abstract

41. Rubin SA, Winer-Muram HT. Thoracic histoplasmosis. J Thorac Imaging 7:39–50, 1992 Abstract

42. Storto ML, Kee ST, Golden JA, et al: Hydrostatic pulmonary edema: High-resolution CT findings. AJR Am J Roentgenol 165:817–820, 1995 Abstract

43. Tanaka N, Matsumoto T, Kuramitsu T, et al: High resolution CT findings in community-acquired pneumonia. J Comp Assist Tomogr 20:600–608, 1996

44. Travis WD, Pittaluga S, Lipschik GY, et al: Atypical pathologic manifestations of *Pneumocystis carinii* pneumonia in the acquired immune deficiency syndrome. Review of 123 lung biopsies from 76 patients with emphasis on cysts, vascular invasion, vasculitis, and granulomas. Am J Surg Pathol 14:615–625, 1990 Abstract

45. Webb WR: High resolution lung computed tomography. Normal anatomic and pathologic findings. Radiol Clin North Am 29:1051–1063, 1991 Abstract

46. Wislez M, Cadranel J, Antoine M, et al: Lymphoma of pulmonary mucosa-associated lymphoid tissue: CT scan findings and pathological correlations. Eur Respir J 14:423–429, 1999 Abstract

47. Yousem SA: Histologic spectrum of chronic necrotizing forms of pulmonary aspergillosis. Hum Pathol 28:650–656, 1997 Abstract